Computers in Biology and Medicine 113 (2019) 103418

Contents lists available at ScienceDirect

Computers in Biology and Medicine

journal homepage: http://www.elsevier.com/locate/compbiomed

Augmentation index in the assessment of wave reflections and systolic loading

Mehmet Kaya [a,*], Vignesh Balasubramanian [a], John K-J. Li [b]

[a] Department of Biomedical and Chemical Engineering and Sciences, Florida Institute of Technology, 150 W University Blvd, Melbourne, FL, 32901, USA
[b] Department of Biomedical Engineering, and Robert Wood Johnson Medical School, Rutgers University, The State University of New Jersey, 599 Taylor Road, Piscataway, NJ, 08854, USA

ARTICLE INFO

Keywords:
Wave reflections
Augmentation index
Inflection pressure
Hypertension
Vasodilation

ABSTRACT

Background: Augmentation index (AI_x) is used to quantify the augmented systolic aortic pressure that impedes ventricular ejection. Its use as an index of wave reflections is questionable. We hypothesize that AI_x is quantitatively different from the reflection coefficient under varied physiological conditions.
Methods: 42 datasets of aortic pressure and flow waveforms were obtained during induced hypertension (methoxamine infusion) and vasodilation (nitroprusside infusion) in our mongrel dog experiments ($n = 5$) and from Mendeley data during various interventions (vasoconstrictors, vasodilators, pacing, stimulation, hemorrhage and hemodilution). Wave reflections and principal components of reflection coefficients were computed for comparison to AI_x and heart rate normalized AI_x.
Results: Principal reflection coefficient, Γ_1, increased in hypertension and decreased in vasodilation, hemorrhage and hemodilution. AI_x followed the trend in many cases but was consistently lower than Γ_1 in almost all the subjects. The Bland-Altman analysis also showed that both AI_x and normalized AI_x underestimated Γ_1. The relationship between augmentation index and reflection coefficient was explained by a linear regression model ($r^2 = 0.23$, $p < 0.01$) in which AI_x followed directional changes in Γ_1 and the normalization of AI_x resulted in a linear model that explained less variation in the relationship between AI_x and Γ_1.
Conclusion: AI_x is a reasonable clinical trend indicator, albeit not an accurate surrogate measure of the amount of wave reflections.

1. Introduction

Hypertension has been recognized as a silent killer that precipitates many forms of cardiovascular diseases [1,2]. Its associated elevation in blood pressure results in a significantly increased vascular load to left ventricular (LV) ejection [3]. Increased vascular stiffness and pulse wave reflections are the dominant factors associated with the stubborn increase in pressure, particularly the central aortic pressure [4].

The amplification of pressure pulses has been attributed to the in-phase summation of reflected waves arising from structural and geometric nonuniformities [1,5]. Pressure (P) and flow (Q) waveforms measured at any site in the vascular system can be considered as the summation of a forward (P_f), or antegrade, traveling wave and a reflected (P_r), or retrograde, traveling wave:

$$P = P_f + P_r \tag{1}$$

$$Q = Q_f + Q_r \tag{2}$$

P_f and P_r can be resolved as

$$P_f = (P + Q.Z_o)/2 \tag{3}$$

$$P_r = (P - Q.Z_0)/2 \tag{4}$$

where Z_o is the characteristic impedance. Forward and reflected waves can also be resolved in the time domain [6].

Both forward and reflected waves are associated with a modulus and phase that varies with frequency. Their ratio defines the reflection coefficient:

$$\Gamma = \frac{P_r}{P_f} \tag{5}$$

* Corresponding author. 150 W University Blvd, Melbourne, FL, 32901, USA.
E-mail addresses: mkaya@fit.edu (M. Kaya), vbalasubrama2016@my.fit.edu (V. Balasubramanian), johnkjli@soe.rutgers.edu (J. K-J. Li).

https://doi.org/10.1016/j.compbiomed.2019.103418
Received 8 June 2019; Received in revised form 26 August 2019; Accepted 26 August 2019
Available online 27 August 2019

or

$$\Gamma = |\Gamma| \angle \Phi_{\Gamma} \tag{6}$$

Its principle component, Γ_1 has the largest reflection magnitude.

Augmentation index (AI_x) based on central aortic pressure has been widely used to characterize both the increased vascular stiffness and wave reflections [7,8]. The definition of AI_x is based on the ratio of the difference of peak systolic pressure (Ps) and pressure at the inflection point during systolic upstroke (Pi), or the augmented pressure, ΔP to pulse pressure (PP), viz:

$$AI_x = \frac{\Delta P}{PP} \tag{7}$$

where PP=Ps-Pd, is the difference between aortic systolic and diastolic pressures. Pi is identified as the aortic pressure that corresponds to peak aortic flow. This is illustrated in Fig. 1. The augmented pressure, ΔP has been used widely as an index of wave reflections and the change in augmented pressure is considered a proportional response of the changes in the amount of wave reflection [9–12].

Additionally, Pi can be determined from pressure alone, making AI_x not dependent on the ejecting blood flow. The simplicity of calculating AI_x based on aortic pressure waveform alone led to many subsequent approaches aimed at constructing central aortic pressure from noninvasive superficial arterial pressure measurements via applanation tonometry, most commonly from the radial artery, carotid artery or the femoral artery [13–16]. Transfer function approach has been the most popular. We have also introduced a new approach that has yet to be implemented for tonometry applications [17].

The association of hypertension with increased large vessel vascular stiffness has been well recognized. AI_x has also been widely used as an index of vascular stiffness, along with pulse wave velocity (PWV). Increased wave reflection has been shown to increase central aortic pressure [1]. For this reason, AI_x has also been used as an index of wave reflections.

In this study, we hypothesize that AI_x is not equivalent to the reflection coefficient and AI_x consistently underestimates the amount of wave reflections.

2. Materials and methods

2.1. Data collection

First, we performed our experiments that involved simultaneously measured aortic pressure and aortic flow and the details have been reported elsewhere [5]. Mongrel dogs (n = 5) that weighed 22 kg on average were anesthetized intravenously using Nembutal (30 mg kg^{-1}) after the University IACUC approval had been obtained. A left thoracotomy was performed at the fifth intercostal space to facilitate the placement of an electromagnetic flowmeter in the ascending aorta. A Millar catheter-tip pressure transducer was placed at the flow measurement site by advancing the catheter from the femoral artery. Normotensive aortic pressure and aortic flow measurements were taken as control, while hypertensive aortic pressure and flow measurements were recorded after intravenous bolus infusion of methoxamine (2–5 mg ml^{-1}). Subsequently, vasodilation was induced with an intravenous bolus infusion of nitroprusside (50 μg ml^{-1}). Moreover, lead II electrocardiogram was established to record the rhythm of the heart. The measured aortic pressure, aortic flow, and electrocardiogram were later digitized at 100 Hz and then stored in the computer for further analysis. In all, six normotensive, three hypertensive and three vasodilated recordings were obtained covering a wide range of blood pressures and waveforms for further analysis.

In addition to our own collected data, data of canine aortic pressure and flow waveforms published by other researchers on Mendeley data (Mendeley Ltd., London, United Kingdom) were also utilized. Aortic pressure and aortic flow data from three normotensive, five vasoconstricted and five vasodilated dogs were also collected [18–21]. Similarly, four datasets of aortic pressure and aortic flow in dogs whose hearts had been electrically stimulated by a pacemaker were obtained from Patel et al. [22]. Furthermore, four aortic pressure-flow measurements were extracted from Ali et al. [23] in which the dogs had been subjected to electrical stimulation of latissimus dorsi (LD) muscle after cardiomyoplasty (CMP) with or without a vascular delay (VD) procedure performed on them. Two sets of aortic pressure and aortic flow data with expanded plasma were acquired from Dujardin et al. [24,25]. The

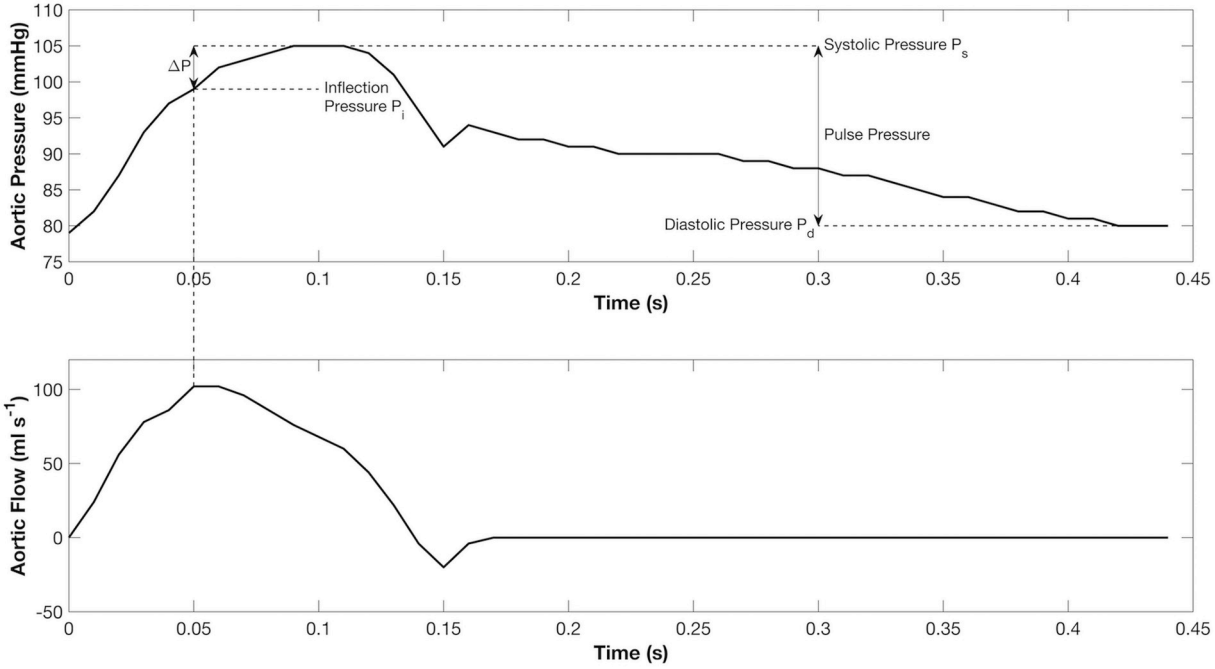

Fig. 1. Definition of Augmentation Pressure Simultaneously recorded aortic pressure and flow waveforms, showing systolic pressure Ps, diastolic pressure Pd, inflection pressure Pi, pulse pressure PP, and augmented pressure ΔP, in defining the augmentation index $AI_y = \Delta P/PP$. Conventional AIx is defined from pressure only by 2nd derivative of pressure to identify Pi.

former was also used to acquire three sets of aortic pressure-flow data under control, fluid infusion and hemorrhage conditions. Aortic pressure-flow data of a stenotic aorta and that of a vascular system that caused diastolic oscillations along with their respective control states were procured from Khir et al. [26] and Fogliardi et al. [27] respectively.

The digitized data were resampled to 100 Hz using a linear interpolation on a 2.6 GHz Intel i5 Processor using Matlab 2017b (The Mathworks Inc., Natick, Massachusetts, USA) and were stored for further analysis. All the datasets were one heartbeat in length and the stored aortic pressure data were then used to identify systolic pressure Ps, diastolic pressure Pd, pulse pressure PP and inflection pressure Pi, in the same heartbeat as defined in Fig. 1 and to resolve the aortic pressure waveform into its forward and reflected components in order to calculate the reflection coefficient. Furthermore, augmentation indices were also calculated only with the pressure based on the method analyzed by Segers et al. [28]. Here, we have used the notation AI_x for augmentation indices that were calculated only with the pressure signal and the notation AI_y for augmentation indices that were calculated from both the pressure and the flow signals.

The calculations were carried out based on the following steps with the same specifications that were used for discrete interpolation:

Step 1. The characteristic impedance of the aorta (Z_o) was calculated by transforming the signals into the frequency domain. The process involved computing the complex coefficients of the frequency components through the Fast Fourier Transform (FFT) algorithm. The computed coefficients were then used to define the characteristic impedance as the average of the absolute value of the ratio of the higher harmonics (3 Hz–10 Hz) of the pressure and the flow signals. Care was taken to make sure that the average was not skewed towards mathematical exceptions from Fourier coefficients by removing outliers using the moving average technique. The results were independently verified before the wave resolution step was performed.

Step 2. The calculated Z_o was used to resolve the pressure signal into its forward or antegrade traveling wave P_f and reflected or retrograde traveling wave P_r, using equations (3) and (4).

Step 3. The resolved pressure components were then utilized to compute reflection coefficient which was defined as the absolute value of the ratio of the fundamental (first) harmonic of the reflected wave to that of the forward wave as in equation (5).

Step 4. A linear search algorithm was employed to find the peak of the flow signal. The index of the peak was then used to record the inflection pressure P_i. Systolic pressure P_s was recorded by employing the linear search algorithm on the pressure signal samples. The algorithm involved comparing each sample with a designated maximum sample. The designated sample was taken as the first sample and it was updated every time a new maximum was found. At the end of the linear search, the designated sample would be the maximum of the entire signal. The diastolic pressure P_d was recorded as the amplitude of the last pressure sample. Augmentation Index AI_y was then calculated as the ratio of ΔP and PP as described in equation (7). Similarly, the second derivative of the pressure waves was calculated and the first two zero-crossings were found using a linear search algorithm and median of the time between the zero-crossings was stored as the inflection point. Then, the inflection pressure was used to calculate AI_x similar to the calculation of AI_y.

Furthermore, the calculated augmentation indices were normalized with respect to heart rate to make the indices independent of peripheral resistance changes [29]. The augmentation indices were normalized to heart rate based on a linear regression of the augmentation indices and the heart rate data that we had collected. The regression equation was then used to find the difference component that normalizes the augmentation indices to 100 beats per minute by the following equations.

$$AI_y = 0.4149 + 0.0017 \times HR \quad (8)$$

$$AI_x = 0.482 + 5.004e^{-4} \times HR \quad (9)$$

2.2. Statistics

Based on the initial 12 datasets we collected, the overall difference between AI_y and Γ_1 had a statistical power of 95% for 15 datasets and we ended up collecting 30 more datasets from the literature. The collected data were classified into four groups viz. normal, vasoconstriction, vasodilation, and pacing. The groups had 12, 8, 12 and 8 datasets respectively. Systolic Augmented pressures were then calculated based on both reflected wave and inflection pressure and were tested for significant differences by subjecting each group to a paired *t*-test that tails to the right. Similarly, systolic forward amplitude and inflection pressure were tested for significant differences by subjecting each group to a paired *t*-test that tail to the left. Both the comparisons were also tested for significance using paired t-tests so that the effects in both directions are known to the readers. Moreover, Bland-Altman analyses were performed to interpret the results [30]. The collected augmentation index AI_x and reflection coefficient Γ_1 data were then subjected to a one-way ANOVA test along with the Tukey-Kramer method for post-hoc analysis to quantify significant differences. Normality tests for the datasets were performed using the Lilliefors test with the null hypothesis that the data were normally distributed. Lilliefors test was chosen since the expected value of the underlying population mean and standard deviation were unknown before data analysis. Furthermore, a least-squares linear regression model was developed to model the relationship between AI_x and Γ_1 and Bland-Altman analysis was performed to interpret how much augmentation index agrees with the actual reflection coefficient that has been defined in the literature. The significance sought for the statistical methods was 95% confidence level. Two of the datasets could not be grouped under any of the 4 groups. However, they were included in, Bland Altman analysis and regression model analysis. Similarly, Bland Altman analysis and regression model analysis were performed between the normalized augmentation index and the reflection coefficient. Moreover, one-way ANOVA was performed on normalized augmentation indices. Besides, correlates of AI_y were computed based on Sherman et al. [31], to find the parameters that vary with AI_y other than the reflection coefficient. The correlates that had been included were the reflection coefficient, arterial reservoir pressure, ejection period and heart rate.

3. Results

Representative pressure waveform that shows augmented pressure under normotensive control conditions is shown in Fig. 2. The reflection amplitude means were significantly higher than the augmented pressure means under normal (M: 6.79 and SD: 3.62 mmHg vs M: 4.23 and SD: 2.31 mmHg, $p = 0.025$) and vasodilated (M: 4.57 and SD: 2.96 mmHg vs M: 2.36 and SD: 3.00 mmHg, $p = 0.042$) conditions while there was no significant difference under induced hypertension (M: 10.48 and SD: 7.02 mmHg vs M: 9.77 and SD: 6.52 mmHg, $p = 0.419$) and pacing conditions (M: 8.80 and SD: 9.48 mmHg vs M: 13.06 and SD: 16.56 mmHg, $p = 0.731$) compared to reflection amplitude. The two-tailed *t*-test results between reflection amplitudes and augmented pressures indicated there were no significant differences under normal (0.053), vasoconstricted (0.837), vasodilated ($p = 0.083$) and pacing ($p = 0.541$) conditions. However, forward amplitude means were not significantly lower than inflection pressure means under normal ($p = 0.489$), vasodilated ($p = 0.521$), vasoconstricted ($p = 0.499$) and pacing conditions ($p = 0.730$). The two-tailed tests between the considered variables resulted in insignificant differences under all

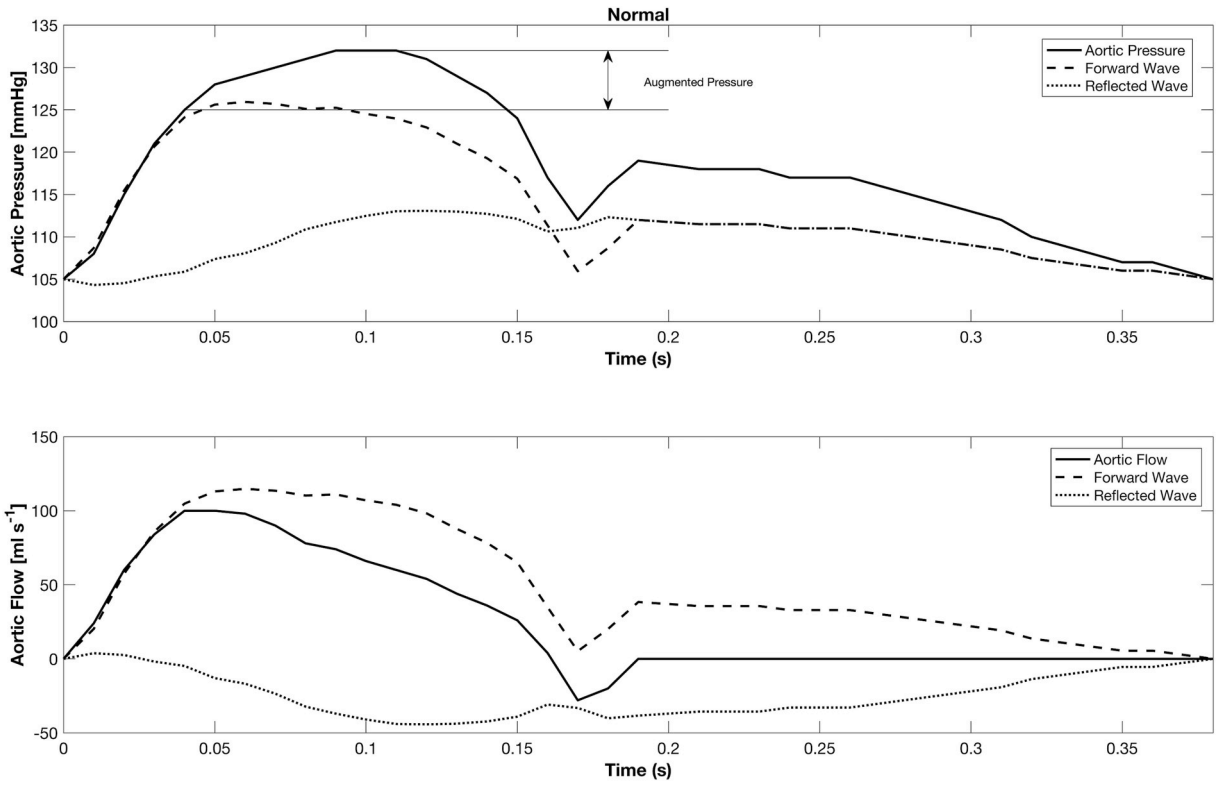

Fig. 2. Resolution of Pressure and Flow waveforms Representative pressure and flow waveforms resolved into their forward and reflected components under normotensive control conditions. Augmented pressures are also shown.

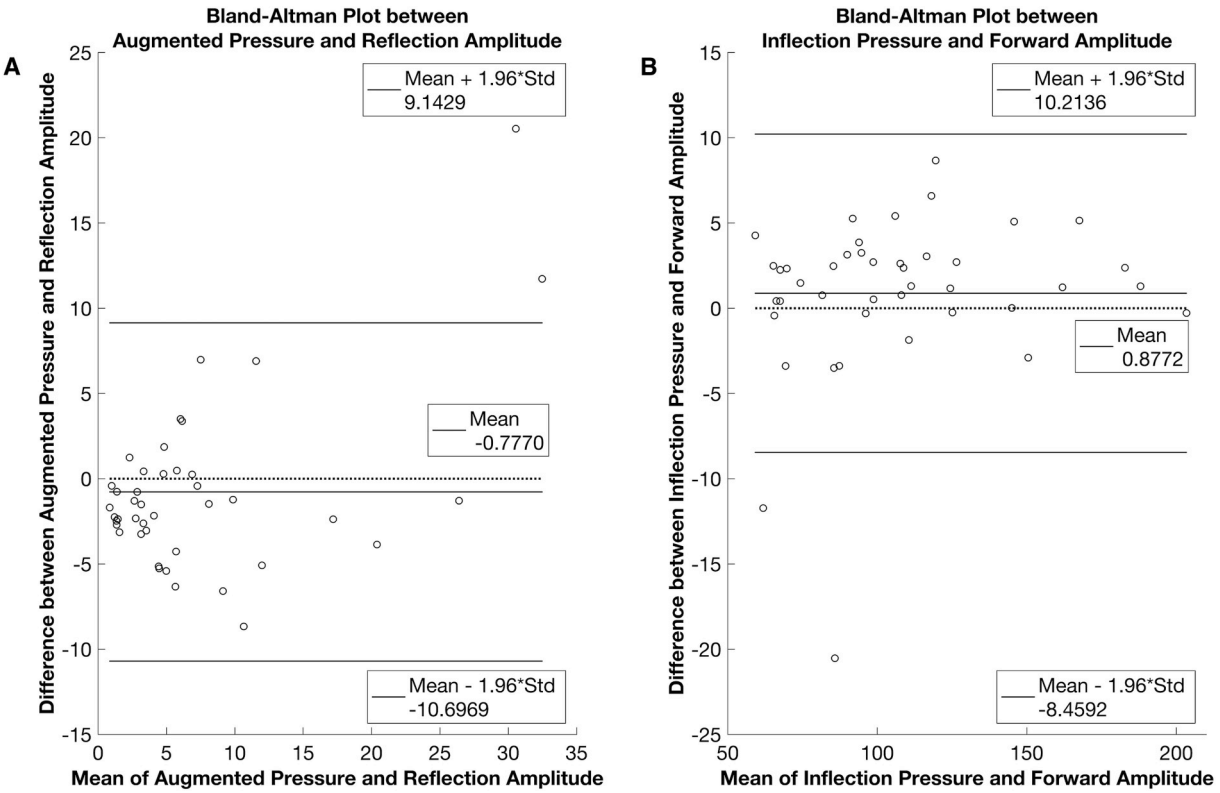

Fig. 3. Bland Altman Analyses of parameters that are used to calculate Augmentation Index and Reflection Coefficient A) Bland Altman analysis of Augmented Pressure (ΔP) calculated from the flow wave and Reflection Amplitude (P_r at P_s) **B)** Bland Altman analysis of Inflection Pressure (P_i) calculated from the flow wave and Forward Amplitude (P_f at P_s).

conditions (normal: $p = 0.977$, vasoconstriction: $p = 0.958$, vasodilation: $p = 0.999$ and pacing: $p = 0.541$).

The normality test of augmented pressure and reflection amplitude differences and inflection pressure and forward amplitude differences rejected the null hypothesis. Bland-Altman analysis of augmented pressure and reflection pressure showed a mean difference of −0.777. Similarly, Bland-Altman analysis of inflection pressure and forward amplitude showed a mean difference of 0.877. These plots indicated that augmented pressure was underestimated compared to reflection pressure and that inflection pressure was overestimated compared to forward amplitude (Fig. 3).

Table 1 shows the reflection coefficient and the augmentation index of all datasets. Augmentation index that was calculated based on both pressure and flow or AI_y was lower than the reflection coefficient in all the subjects except three datasets from the pacing group. Moreover, the augmentation indices were either close to or equal to zero in 16 subjects when the reflection coefficients were greater than zero because the inflection pressures were close to their systolic pressures making ΔP close to zero. The normality test failed to reject the null hypothesis for AI_y of all the groups and Γ_1 of normotensive and vasoconstricted groups while the normality test accepted the null hypothesis for AI_y of the vasodilation group and the pacing group. One-way ANOVA test resulted in significant differences in AI_y between the normal and the pacing groups ($p = 0.004$) and between the vasodilation and the pacing groups ($p < 0.001$). There were no other significant differences among the 4 groups. In the case of Γ_1, there were significant differences between the normal and the vasoconstriction groups ($p = 0.009$), the vasoconstriction and the vasodilation groups ($p < 0.001$) and the vasodilation and the pacing groups ($p = 0.043$). There were no other significant differences among the 4 groups. Augmentation indices AI_x and AI_y differ by a mean value of 0.100. The normality test failed to reject the null hypothesis for AI_x under normotensive and pacing conditions and the test accepted the null hypothesis for AI_x under vasoconstricted and vasodilated conditions. ANOVA results indicated that there were no significant differences among the groups.

The normality test of differences between AI_x and Γ_1 rejected the null hypothesis with $p = 0.022$. Bland-Altman analysis revealed a bias line that lied above the 95% confidence interval of the mean difference

Table 1
Summary of pressure parameters in comparison with reflection indices under different conditions.

S. No.	P_s[a] (mmHg)	P_d[b] (mmHg)	PP[c] (mmHg)	P_i[d] (mmHg)	P_i[e] (mmHg)	AI_x[f]	AI_y[g]	Γ_1[h]	Condition
1	120.0	96.0	24.0	120.0	118.0	0.000	0.083	0.504	Normotensive
2	111.0	96.0	15.0	110.0	109.0	0.048	0.095	0.293	Normotensive
3	132.0	105.0	27.0	132.0	125.0	0.000	0.259	0.453	Normotensive
4	114.0	90.0	24.0	114.0	112.0	0.000	0.083	0.458	Normotensive
5	105.0	80.0	25.0	104.0	99.0	0.040	0.240	0.518	Normotensive
6	128.0	103.0	25.0	127.0	125.0	0.040	0.120	0.387	Normotensive
7	156.0	130.0	26.0	151.0	145.0	0.192	0.423	0.556	Methoxamine
8	200.0	155.0	45.0	198.0	184.0	0.044	0.356	0.696	Methoxamine
9	164.0	132.0	32.0	158.0	149.0	0.188	0.469	0.675	Methoxamine
10	96.0	65.0	31.0	87.0	96.0	0.290	0.000	0.067	Nitroprusside
11	83.0	49.0	34.0	79.0	82.0	0.118	0.029	0.150	Nitroprusside
12	102.4	76.0	26.4	98.4	100.0	0.152	0.091	0.226	Nitroprusside
13	115.4	93.5	21.9	114.0	109.6	0.061	0.263	0.387	Normotensive
14	127.8	94.2	33.6	126.3	127.8	0.044	0.000	0.192	Fluid Infusion
15	110.2	84.9	25.3	86.6	110.0	0.933	0.010	0.215	Expanded Plasma
16	86.7	63.0	23.6	67.2	86.6	0.824	0.004	0.195	Hemorrhage
17	68.3	43.4	24.8	68.4	68.2	0.014	0.072	0.612	During pacing
18	68.0	50.5	17.6	68.4	68.0	0.036	0.141	0.548	After pacing
19	69.1	56.3	12.8	68.9	67.3	0.000	0.389	0.496	During pacing
20	70.8	50.5	20.3	70.5	65.2	0.005	0.164	0.108	After pacing
21	72.5	52.8	19.7	72.2	70.9	0.015	0.081	0.410	Normotensive
22	82.4	43.8	38.6	81.3	75.1	0.028	0.190	0.393	Normotensive
23	114.3	43.3	71.0	76.9	95.9	0.527	0.260	0.815	Vasoconstriction
24	93.4	77.7	15.8	93.4	85.6	0.000	0.497	0.586	During LD stimulation without VD
25	91.5	76.5	15.1	91.0	83.7	0.032	0.517	0.573	After LD stimulation without VD
26	116.4	60.2	56.2	116.3	75.6	0.002	0.726	0.598	During LD stimulation with VD
27	94.3	56.0	38.3	92.8	56.0	0.040	1.001	0.762	After LD stimulation with VD
28	64.9	38.9	26.0	59.2	61.3	0.218	0.137	0.700	Nitroprusside
29	96.3	76.7	19.6	96.0	94.4	0.014	0.094	0.886	Methoxamine
30	68.7	36.8	32.0	68.6	68.7	0.003	0.003	0.496	Nitroprusside
31	97.9	77.8	20.1	97.5	96.3	0.018	0.076	0.758	Methoxamine
32	127.2	85.0	42.2	123.1	121.4	0.099	0.138	0.737	Normal
33	214.4	152.0	62.5	209.3	188.7	0.083	0.412	0.752	Occlusion
34	172.0	125.2	46.8	171.6	170.1	0.008	0.040	0.272	Normotensive
35	208.1	154.3	53.8	206.4	203.2	0.033	0.091	0.335	Angiotensin
36	110.9	49.4	61.5	109.6	108.4	0.021	0.040	0.228	Hydralazine
37	91.5	47.0	44.5	91.2	91.5	0.006	0.000	0.239	Nitroprusside
38	73.5	53.4	20.1	73.5	66.5	0.000	0.351	0.410	Vasodilation
39	157.7	121.9	35.8	156.9	148.3	0.023	0.264	0.896	Vasoconstriction
40	171.8	137.9	33.9	167.0	162.6	0.142	0.273	0.559	Expanded Plasma
41	130.2	87.3	42.9	128.2	123.9	0.046	0.147	0.462	Normal
42	111.0	90.4	20.6	108.1	108.7	0.140	0.111	0.373	Diastolic Oscillations

[a] Systolic Pressure.
[b] Diastolic Pressure.
[c] Pulse Pressure.
[d] Inflection Pressure calculated from pressure only.
[e] Inflection Pressure calculated from flow signal.
[f] Augmentation Index calculated from pressure only.
[g] Augmentation Index calculated from flow signal.
[h] Reflection Coefficient.

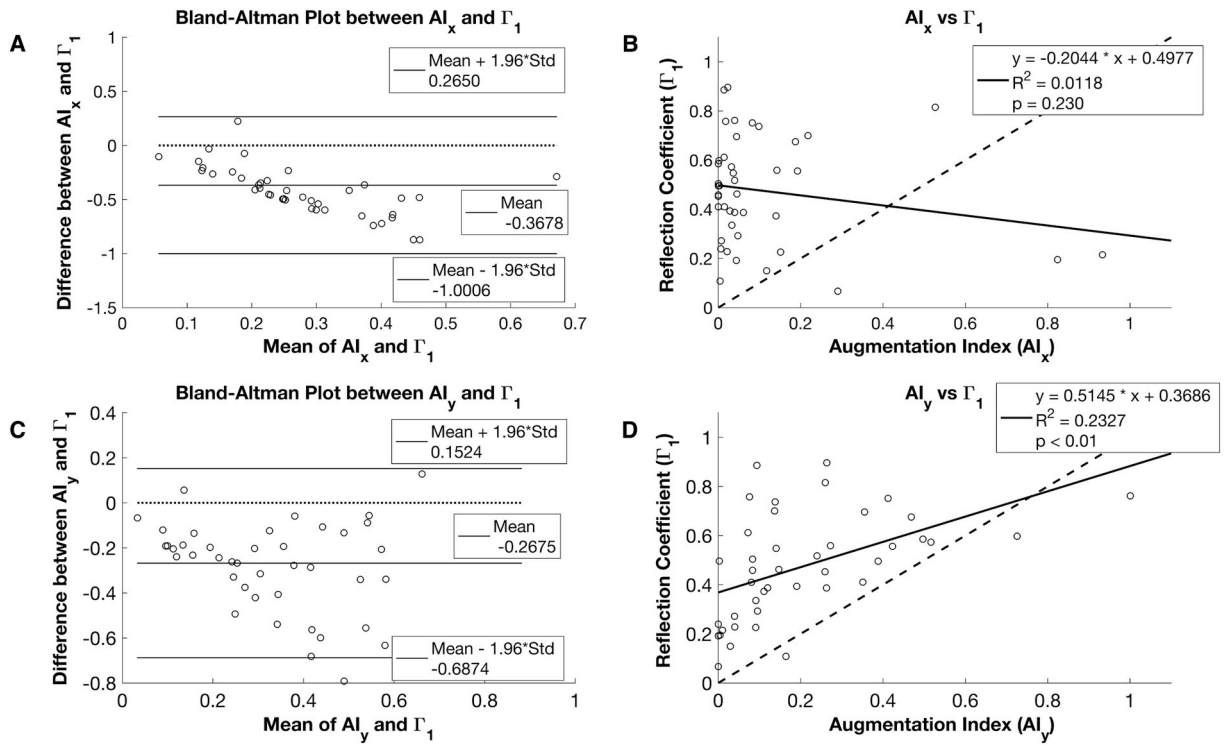

Fig. 4. Analysis of the relationship between Augmentation Index and Reflection Coefficient A) Bland-Altman analysis of Augmentation Index (AI_x) that was calculated from the pressure wave only and Reflection Coefficient (Γ_1) **B)** Linear regression model that predicts reflection coefficient (Γ_1) from augmentation index (AI_x) that was calculated from the pressure wave only. Dotted line is the line of identity when AI_x equals Γ_1. It is clear that AI_x largely underestimates Γ_1. **C)** Bland-Altman analysis of Augmentation Index (AI_y) that was calculated from both the flow and the pressure waves and Reflection Coefficient (Γ_1) **D)** Linear regression model that predicts reflection coefficient (Γ_1) from augmentation index (AI_y) that was calculated from both the flow and the pressure waves. Dotted line is the line of identity when AI_y equals Γ_1. It is clear that AI_y also largely underestimates Γ_1.

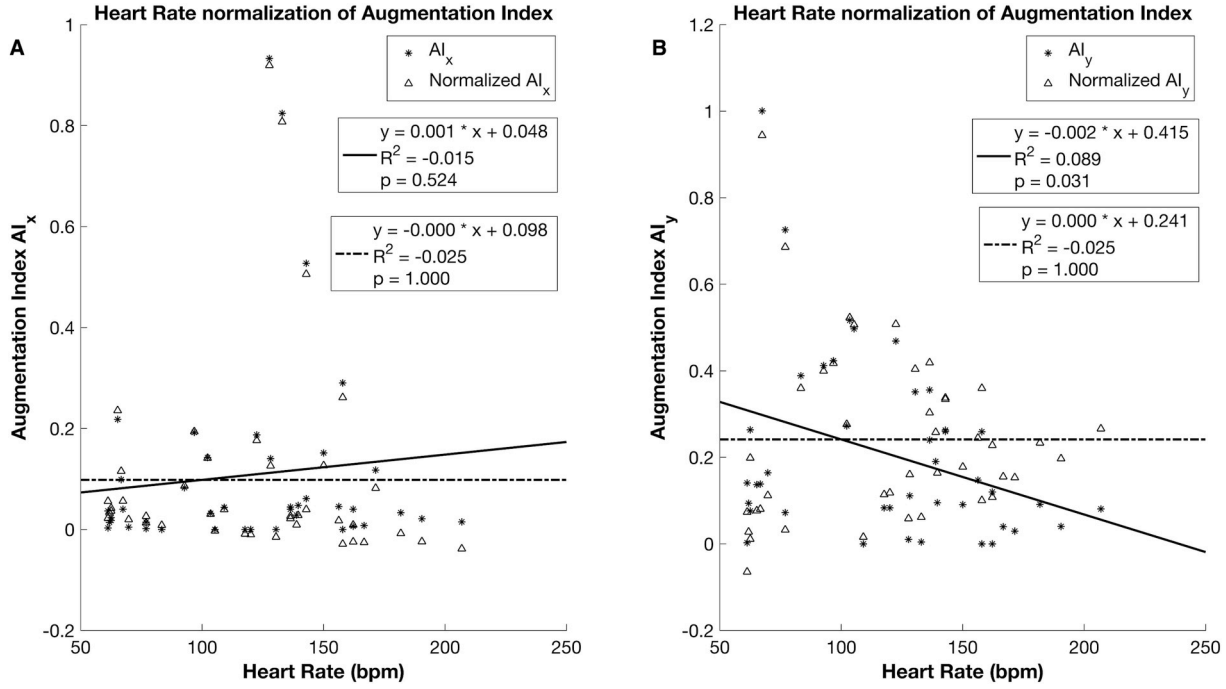

Fig. 5. Heart Rate Normalization of Augmentation Index A) Scatter plot of Augmentation Index (AI_x) that was calculated from pressure wave only and the corresponding normalized Augmentation Index (AI_x) with Heart Rate as the reference. The solid line represents the regression line between AI_x and heart rate, and the dashed line represents the regression line between normalized AI_x and heart rate. **B)** Scatter plot of Augmentation Index (AI_y) that was calculated from pressure and flow waves and the corresponding normalized Augmentation Index (AI_y) with Heart Rate as the reference. The solid line represents the regression line between AI_y and heart rate, and the dashed line represents the regression line between normalized AI_y and heart rate.

between AI_x and Γ_1 (Fig. 4A). This showed that the reflections were underestimated. The linear model (Fig. 4B) that was used to explain the relationship between AI_x and Γ_1 explained only 1.18% of the variation between the variables and it was not significant compared to a zero-slope model ($p = 0.230$). The normality test of the differences between AI_y and Γ_1 failed to reject the null hypothesis with $p = 0.244$. A Bland-Altman analysis of AI_y and Γ_1 revealed a bias line that lied above the 95% confidence interval of the mean difference between AI_y and Γ_1 (see Fig. 4C). This showed that AI_y underestimates the actual reflections even when the flow signals were used to compute the augmentation index. The relationship between augmentation index and reflection coefficient was explained by a linear regression model (Fig. 4D). The constant term in the regression equation revealed that the reflection coefficient was on average 0.369 when the augmentation index was zero due to zero or very small ΔP. The model accounted for 23.27% of the variation between AI_x and Γ_1 (adjusted $R^2 = 0.233$) and the model was significant in comparison to a zero-slope model ($p < 0.01$).

Fig. 5 shows the calculated augmentation indices along with the normalized indices along with their regression lines. The normality test of the normalized AI_x failed to reject the null hypothesis for the normotensive and the vasoconstricted groups while the normality test rejected the null hypothesis for the vasodilated and pacing groups. One-way ANOVA revealed that there were no significant differences among the groups. The normality test of the differences between the normalized AI_x and Γ1 rejected the null hypothesis with $p = 0.003$. Bland-Altman analysis of the normalized AI_x and Γ_1 revealed that the bias line lied above the 95% confidence interval of the mean difference line (see Fig. 6A). This showed that the normalization of AI_x still underestimated the reflections. The linear model that was generated to explain the variations between normalized AI_x and Γ_1 resulted in a model that is not significantly different from a zero-slope model (Fig. 6B). The normality test of the normalized AI_y failed to reject the null hypothesis. One-way ANOVA resulted in insignificant differences among all the groups. The normality test of the differences between normalized AI_y and Γ_1 rejected the null hypothesis with $p = 0.001$. Bland-Altman analysis revealed that the bias line lied above the 95% confidence interval of the mean difference between normalized AI_y and Γ_1 (see Fig. 6C) which shows that the normalized AI_y also underestimates the actual reflections even when the flow waves are used to calculate AI_y. The linear regression model (Fig. 6D) revealed that the reflection coefficient was 0.342 when the normalized AI_y was low due to low ΔP on average. The model accounted for 7.81% of the variation between the normalized AI_y and Γ_1 and the model was statistically significant compared to a zero-slope model (p-value = 0.017). Analysis of correlates showed that the AI_y that was not normalized with heart rate had the highest correlation value with augmented reservoir pressure ($r = 0.794$, $p < 0.001$). The correlates in decreasing order of strength are reflection coefficient ($r = 0.501$, $p < 0.001$), ejection period ($r = 0.382$, $p = 0.013$) and heart rate ($r = -0.333$, $p = 0.031$).

4. Discussion

Conditions that pertain to increase systemic blood pressure generally tend to increase vascular stiffness, wave reflections and augmented pressure. In this study, the augmentation index has been calculated from a variety of scenarios under which the arterial system was either vasoconstricted or vasodilated due to the action of pharmaceutical agents or homeostatic compensation. Here, we have computed augmentation indices using both aortic pressure and flow signals (AI_y) and the pressure signal only (AI_x). Furthermore, the corresponding reflection coefficient

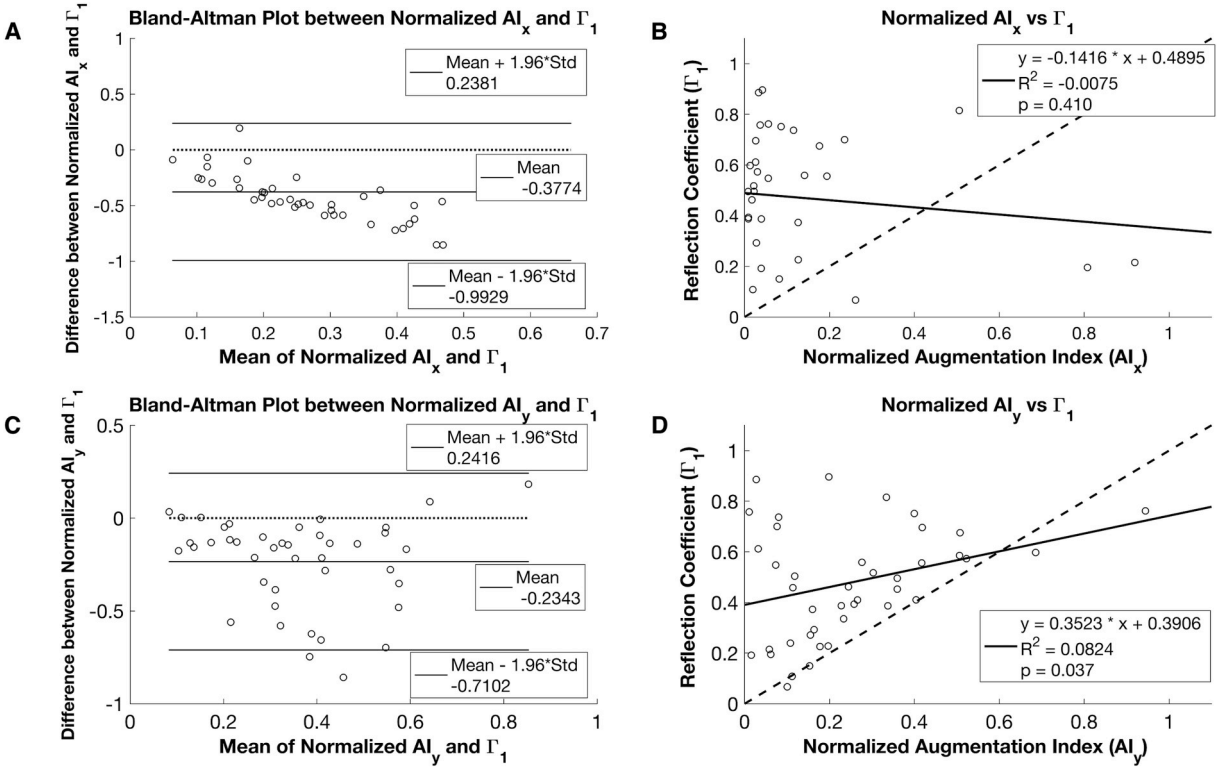

Fig. 6. Analysis of the relationship between Heart Rate normalized Augmentation Index and Reflection Coefficient A) Bland-Altman analysis of normalized Augmentation Index (AI_x) that was calculated from the pressure wave only and Reflection Coefficient (Γ_1) **B)** Linear regression model that predicts reflection coefficient (Γ_1) from normalized augmentation index (AI_x) that was calculated from the pressure wave only. Dotted line is the line of identity when normalized AI_x equals Γ_1. It is clear that normalized AI_x largely underestimates Γ_1. **C)** Bland-Altman analysis of normalized Augmentation Index (AI_y) that was calculated from both the flow and the pressure waves and Reflection Coefficient (Γ_1) **D)** Linear regression model that predicts reflection coefficient (Γ_1) from normalized augmentation index (AI_y) that was calculated from both the flow and the pressure waves. Dotted line is the line of identity when normalized AI_y equals Γ_1. It is clear that normalized AI_y also largely underestimates Γ_1.

was calculated for comparison. A Bland-Altman analysis (see Fig. 4A and C) and a visual inspection of the AI_x and AI_y data (see Table 1) showed that the augmentation index, in general, underestimated wave reflections.

The disparity between AI_x and Γ_1 has been explained below. The inflection pressure, which is the pressure at which aortic flow is maximum during a cardiac cycle, is close to the peak systolic pressure, particularly under vasodilated and normal conditions. However, a linear model between augmentation index with reflection coefficient shows that AI_y has a strong relationship with Γ_1 (see Figs. 4D and 6D). Previous researches have used the change in augmented pressure as an indicator of change in wave reflections [4,7–12]. We have shown here that the proportional changes in AI_x or AI_y differ from the reflection coefficient or the fraction of the propagating wave that is reflected. These reflections are locally dispersed in space and time that contribute to the reflection coefficient through its wave resolution process. Meanwhile, when AI_x is calculated with its current definition, the lack of complete underlying information on the wave dispersion phenomenon makes it an inadequate marker of wave reflections.

Normalization of the augmentation index with respect to the heart rate did not improve the results and further analysis reveals that even normalized AI_x still underestimates the central reflections (see Fig. 6) A recent review has shed light on how serial elevation in the heart rate over prolonged time courses requires careful attention when augmentation indices are calculated [32]. In addition to heart rate, our data also showed that augmentation index was strongly correlated to the ejection period and peak systolic pressure. Our AI_y data were also correlated with the ejection period. The change in different pressure states affects the ejection period which is related to the temporal overlapping of forward and reflection waves [33]. Besides, a recent computational modeling study has revealed that variations in augmentation index depend on both cardiac and vascular functions while the reflection parameter depends on only vascular parameters [34]. The authors showed that changes in left ventricular stroke work did not necessarily change AI_x while wave reflections are affected by stroke work under a variety of scenarios. We have previously shown that hypertensive and vasodilation mechanisms severely affect the left ventricular stroke work and that these changes can be tracked by computing wave reflection parameters [5]. Our present results also indicate that both AI_x and AI_y are significantly different under hypertensive and vasodilated conditions compared to the normotensive scenario. These correlations indicate that a simple heart rate normalization will not be enough to capture the reflection phenomenon with the current definition of AI_x.

Several studies have shown that AI_x is a good predictor of outcome in specific groups of patients such as those with acute ischemic stroke [35], end-stage renal failure [36] and those who undergo percutaneous coronary interventions [2]. However, AI_x has also been shown to be a less suitable measure of stiffness in the elderly [37] and type 2 diabetic patient groups [38]. Our data also showed a trend among the different groups. A true index of the augmentation phenomenon would differentiate the hypertension group from the normal group and the vasodilated group from the hypertension group as the reflection coefficient identifies significant differences in means. Even though the difference in AI_y means among the normal, the vasoconstriction and the vasodilation groups were not significant, the data followed a trend of increased AI_y under vasoconstriction and decreased AI_y under vasodilation in comparison with the normotensive group. To sum up all the AI_x related results, AI_x is not an accurate surrogate measure of wave reflections.

A recent study [39] on the validity of measuring augmentation index showed that the measurements of AI_x were highly reliable in terms of determining them using a cuff-based pressure measurement method. It must be noted that the validation of these indices was based on brachial artery pressure measurements and the computations of the augmentation index and the reflection coefficient in our study have been based on central blood pressure measurements. It must also be acknowledged that there is a requirement for the broader consensus of the value of central blood pressure measurements [40]. However, the use of central blood pressure as an indicator of characteristic aortic impedance and arterial compliance has interesting applications in estimating arterial stiffness. With the advent of non-invasive peripheral pressure signal measurement techniques, the scope of AI_x can be extended by converting the peripheral pressure measurements into central pressure values with the use of patient-specific transfer function techniques. These values can be further used to compute non-linear compliance as defined in Kaya et al. [41] and the reflection measures as calculated in the present study, can be used to define a new augmentation index that does not underestimate arterial stiffness. With such a device, the timing of the reflected wave [42] can be used as an indicator of the effects of pharmacological agents on diseased states such as isolated hypertension and heart failure. One of the other major applications that the authors foresee is the use of probabilistic learning techniques such as naive Bayes or logistic regression to compute pathophysiology states along with computations that we have done in our previous studies [5,41]. For example, with access to routine data collection during catheterization and blood flow estimation techniques, the parameters that we have calculated can be utilized to classify different disease states that a set of simple regression models cannot predict.

One of the limitations of this study is the heterogeneity of data. The methods used to constrict or dilate the arteries were different for different datasets since they had been collected from a variety of studies. However, the datasets that have been used in the study are heterogeneous and they help understand why AI_x is underestimated under a variety of clinical scenarios.

Grants

This research did not receive any specific grant from funding agencies in the public, commercial or not-for-profit sectors.

Disclosures

The authors report no relationships that could be construed as conflict of interest.

Acknowledgments

None.

References

[1] J.K.-J. Li, Dynamics of the Vascular System and Interaction with the Heart, second ed., World Scientific, Singapore, 2018.
[2] T. Weber, J. Auer, M.F. O'Rourke, E. Kvas, E. Lassnig, G. Lamm, N. Stark, M. Rammer, B. Eber, Increased arterial wave reflections predict severe cardiovascular events in patients undergoing percutaneous coronary interventions, Eur. Heart J. 26 (2005) 2657–2663, https://doi.org/10.1093/eurheartj/ehi504.
[3] J.K.-J. Li, The Arterial Circulation: Physical Principles and Clinical Applications, Springer, New York, 2000.
[4] A.P. Avolio, L.M. Van Bortel, P. Boutouyrie, J.R. Cockcroft, C.M. McEniery, A. D. Protogerou, M.J. Roman, M.E. Safar, P. Segers, H. Smulyan, Role of pulse pressure amplification in arterial hypertension, Hypertension 54 (2009) 375–383, https://doi.org/10.1161/HYPERTENSIONAHA.109.134379.
[5] M. Kaya, V. Balasubramanian, Y. Ge, J.K.-J. Li, Energetically wasteful wave reflections due to impedance mismatching in hypertension and their reversal with vasodilator: time and frequency domain evaluations, Comput. Biol. Med. 104 (2019), https://doi.org/10.1016/j.compbiomed.2018.11.014.
[6] J.K.-J. Li, Time domain resolution of forward and reflected waves in the aorta, IEEE Trans. Biomed. Eng. 33 (1986) 783–785, https://doi.org/10.1109/TBME.1986.325903.
[7] R.E.D. Climie, S.B. Nikolic, P. Otahal, L.J. Keith, J.E. Sharman, Augmentation index and arterial stiffness inpatients with type 2 diabetes mellitus, Artery Res. 7 (2013) 194–200, https://doi.org/10.1016/j.artres.2013.09.002.
[8] A.N. Gurovich, W.W. Nichols, R.W. Braith, C.R. Conti, Patients with refractory angina have increased aortic wave reflection and wasted left ventricular pressure energy, Artery Res. 8 (2014) 9–15, https://doi.org/10.1016/j.artres.2014.01.003.
[9] P. Segers, J. De Backer, D. Devos, S.I. Rabben, T.C. Gillebert, L.M. Van Bortel, J. De Sutter, A. De Paepe, P.R. Verdonck, Aortic reflection coefficients and their association with global indexes of wave reflection in healthy controls and patients

with Marfan's syndrome, Am. J. Physiol. Cell Physiol. 290 (2006) H2385–H2392, https://doi.org/10.1152/ajpheart.01207.2005.
[10] M. Namasivayam, B.J. McDonnell, C.M. McEniery, M.F. O'Rourke, Does wave reflection dominate age-related change in aortic blood pressure across the human life span? Hypertension 53 (2009) 979–985, https://doi.org/10.1161/HYPERTENSIONAHA.108.125179.
[11] W.W. Nichols, B.M. Singh, Augmentation index as a measure of peripheral vascular disease state, Curr. Opin. Cardiol. 17 (2002) 543–551, https://doi.org/10.1097/00001573-200209000-00016.
[12] A.A. Torjesen, N. Wang, M.G. Larson, N.M. Hamburg, J.A. Vita, D. Levy, E. J. Benjamin, R.S. Vasan, G.F. Mitchell, Forward and backward wave morphology and central pressure augmentation in men and women in the framingham heart study, Hypertension 64 (2014) 259–265, https://doi.org/10.1161/HYPERTENSIONAHA.114.03371.
[13] J.D. Cameron, B.P. Mcgrath, A.M. Dart, Use of radial artery applanation tonometry and a generalized transfer function to determine aortic pressure augmentation in subjects with treated hypertension, J. Am. Coll. Cardiol. 32 (1998) 1214–1220, https://doi.org/10.1016/S0735-1097(98)00411-2.
[14] C.H. Chen, E. Nevo, B. Fetics, P.H. Pak, F.C.P. Yin, W.L. Maughan, D.A. Kass, Estimation of Central aortic pressure waveform by mathematical transformation of radial tonometry pressure: validation of generalized transfer function, Circulation 95 (1997) 1827–1836, https://doi.org/10.1161/01.CIR.95.7.1827.
[15] C.H. Chen, C.T. Ting, A. Nussbacher, E. Nevo, D.A. Kass, P. Pak, S.P. Wang, M. S. Chang, F.C.P. Yin, Validation of carotid artery tonometry as a means of estimating augmentation index of ascending aortic pressure, Hypertension 27 (1996) 168–175, https://doi.org/10.1161/01.HYP.27.2.168.
[16] M. Dhindsa, J.N. Barnes, A.E. DeVan, J. Sugawara, H. Tanaka, Comparison of augmentation index derived from multiple devices, Artery Res. 5 (2011) 112–114, https://doi.org/10.1016/j.artres.2011.06.002.
[17] A. Patel, J.K.-J. Li, B. Finegan, M. McMurtry, Aortic pressure estimation using blind identification approach on single input multiple output non-linear Wiener systems, IEEE Trans. Biomed. Eng. 65 (2017), https://doi.org/10.1109/TBME.2017.2688425, 1–1.
[18] R. Burattini, S. Natalucci, K.B. Campbell, Viscoelasticity modulates resonance in the terminal aortic circulation, Med. Eng. Phys. 21 (1999) 175–185, https://doi.org/10.1016/S1350-4533(99)00041-7.
[19] G. Gnudi, New closed-form expressions for the estimation of arterial windkessel compliance, Comput. Biol. Med. 28 (1998) 207–223, https://doi.org/10.1016/S0010-4825(98)00008-0.
[20] M. Higashidate, K. Tamiya, T. Beppu, Y. Imai, Regulation of the aortic valve opening. In vivo dynamic measurement of aortic valve orifice area, J. Thorac. Cardiovasc. Surg. 110 (1995) 496–503, https://doi.org/10.1016/S0022-5223(95)70246-6.
[21] J.J. Wang, J.C. Bouwmeester, I. Belenkie, N.G. Shrive, J.V. Tyberg, Alterations in aortic wave reflection with vasodilation and vasoconstriction in anaesthetized dogs, Can. J. Cardiol. 29 (2013) 243–253, https://doi.org/10.1016/j.cjca.2012.03.001.
[22] B.G. Patel, S.H. Shah, L.I. Astra, R.L. Hammond, Z.A. Sharif, P.J. McDonald, L. W. Stephenson, Skeletal muscle ventricle aortic counterpulsation: function during chronic heart failure, Ann. Thorac. Surg. 73 (2002) 588–593, https://doi.org/10.1016/S0003-4975(01)03458-0.
[23] A.T. Ali, W.P. Santamore, B.Y. Chiang, R.D. Dowling, G.R. Tobin, A.D. Slater, Vascular delay of the Latissimus dorsi provides an early hemodynamic benefit in dynamic cardiomyoplasty, Ann. Thorac. Surg. 67 (1999) 1304–1311, https://doi.org/10.1016/S0003-4975(99)00186-1.
[24] J.P. Dujardin, D.N. Stone, Characteristic impedance of the proximal aorta determined in the time and frequency domain: a comparison, Med. Biol. Eng. Comput. 19 (1981) 565–568, https://doi.org/10.1152/ajpheart.1984.246.1.H1.
[25] J.P. Dujardin, D.N. Stone, L.T. Paul, H.P. Pieper, Response of systemic arterial input impedance to volume expansion and hemorrhage, Am. J. Physiol. 238 (1980) H902–H908.
[26] A.W. Khir, K.H. Parker, Wave intensity in the ascending aorta: effects of arterial occlusion, J. Biomech. 38 (2005) 647–655, https://doi.org/10.1016/j.jbiomech.2004.05.039.
[27] R. Fogliardi, M. di Donfrancesco, R. Burattini, Comparison of linear and nonlinear formulations of the three-element windkessel model, Am. J. Physiol. Cell Physiol. 271 (1996) H2661–H2668.
[28] P. Segers, E.R. Rietzschel, M.L. De Buyzere, D. De Bacquer, L.M. Van Bortel, G. De Backer, T.C. Gillebert, P.R. Verdonck, Assessment of pressure wave reflection: getting the timing right!, Physiol. Meas. (2007), https://doi.org/10.1088/0967-3334/28/9/006.
[29] I.B. Wilkinson, H. MacCallum, L. Flint, J.R. Cockcroft, D.E. Newby, D.J. Webb, The influence of heart rate on augmentation index and central arterial pressure in humans, J. Physiol. 525 (2000) 263–270, https://doi.org/10.1111/j.1469-7793.2000.t01-1-00263.x.
[30] J.M. Bland, D.G. Altman, Statistical methods for assessing agreement between two methods of clinical measurement, Lancet 327 (1986) 307–310.
[31] J.E. Sharman, J.E. Davies, C. Jenkins, T.H. Marwick, Augmentation index, left ventricular contractility, and wave reflection, Hypertension 54 (2009) 1099–1105, https://doi.org/10.1161/HYPERTENSIONAHA.109.133066.
[32] L. Stoner, J. Faulkner, A. Lowe, D. M.L, J. M.Y, R. Love, S.R. D, Should the augmentation index be normalized to heart rate? J. Atheroscler. Thromb. 21 (2014) 11–16. DN/JST.JSTAGE/jat/20008 [pii].
[33] G.F. Mitchell, Y. Lacourcière, J.M.O. Arnold, M.E. Dunlap, P.R. Conlin, J.L. Izzo, Changes in aortic stiffness and augmentation index after acute converting enzyme or vasopeptidase inhibition, Hypertension 46 (2005) 1111–1117, https://doi.org/10.1161/01.HYP.0000186331.47557.ae.
[34] M.H.G. Heusinkveld, T. Delhaas, J. Lumens, W. Huberts, B. Spronck, A.D. Hughes, K.D. Reesink, Augmentation index is not a proxy for wave reflection magnitude: mechanistic analysis using a computational model, J. Appl. Physiol. (2019), https://doi.org/10.1152/japplphysiol.00769.2018.
[35] R.L. Soiza, M.M. Davie, D.J.P. Williams, Use of the augmentation index to predict short-term outcome after acute ischemic stroke, Am. J. Hypertens. 23 (2010) 737–742, https://doi.org/10.1038/ajh.2010.66.
[36] G.M. London, J. Blacher, B. Pannier, A.P. Guerin, S.J. Marchais, M.E. Safar, in: Arterial Wave Reflections and Survival in End-Stage Renal Failure, vol. 38, 2001, pp. 434–438.
[37] F. Fantin, A. Mattocks, C.J. Bulpitt, W. Banya, C. Rajkumar, Is augmentation index a good measure of vascular stiffness in the elderly? Age Ageing 36 (2007) 43–48, https://doi.org/10.1093/ageing/afl115.
[38] P. Lacy, D.G. O'Brien, A.G. Stanley, M.M. Dewar, P.P. Swales, B. Williams, Lncreased pulse wave velocity is not associated with elevated augmentation index in patients with diabetes, J. Hypertens. 22 (2004) 1937–1944.
[39] M.-H. Hwang, J.-K. Yoo, H.-K. Kim, C.-L. Hwang, K. Mackay, O. Hemstreet, W. Nichols, D. Christou, Validity and reliability of aortic pulse wave velocity and augmentation index as determined by the new cuff-based SphygmoCor Xcel, J. Hum. Hypertens. 28 (2014) 475–481.
[40] R.R. Townsend, C. Rosendorff, W.W. Nichols, D.G. Edwards, J.A. Chirinos, B. Fernhall, W.C. Cushman, American Society of Hypertension position paper: central blood pressure waveforms in health and disease, J. Am. Soc. Hypertens. 10 (2016) 22–33, https://doi.org/10.1016/j.jash.2015.10.012.
[41] M. Kaya, V. Balasubramanian, A. Patel, Y. Ge, J.K.-J. Li, A novel compliance-pressure loop approach to quantify arterial compliance in systole and in diastole, Comput. Biol. Med. 99 (2018) 98–106, https://doi.org/10.1016/j.compbiomed.2018.06.001.
[42] C.F. Liao, H.M. Cheng, S.H. Sung, W.C. Yu, C.H. Chen, Determinants of pressure wave reflection: characterization by the transit time-independent reflected wave amplitude, J. Hum. Hypertens. 25 (2011) 665–671, https://doi.org/10.1038/jhh.2010.106.